[Frontiers in Bioscience 19, 1377-1385, June 1, 2014]

Evaluation of hepatic steatosis using dual-energy CT with MR comparison

Taotao Sun[1] , Xiaozhu Lin[1] ,Kemin Chen[1]

[1]China Department of Radiology, Shanghai Ruijin Hospital, No, 197 Ruijin Er Rd, Shanghai, 200011

TABLE OF CONTENTS

1. ABSTRACT

In this study, we aimed to explore the potential of dual-energy computed tomography (DECT) in evaluating liver fat; we also compared the diagnostic performance of DECT, T1-weighted dual-echo magnetic resonance (MR) imaging, and 1H-MR spectroscopy (1H-MRS) in assessing hepatic steatosis in a fatty liver rat model. Fat (water) concentration measurements by DECT spectral imaging, MR findings, and 1H-MRS measurements of hepatic fat showed similar correlations with the histopathologic results. Furthermore, a good correlation was observed between the fat (water) concentration and 1H-MRS measurements (r = 0.8.00 and P less than 0.0.01). The discriminant accuracies of the fat (water) concentration, MR findings, and 1H-MRS measurements were 66.7, 64, and 56 percent, respectively. Therefore, we conclude that the findings of DECT spectral CT imaging are strongly correlated with histopathologic findings in cases of steatosis; in addition, DECT can allow rapid, accurate evaluations of hepatic steatosis that are as effective as those obtained using T1-weighted dual-echo MR imaging and 1H-MRS.

2. INTRODUCTION

Over the past few years, non-alcoholic fatty liver disease (NAFLD) has become an emerging epidemic in the Western world. NAFLD represents a disease spectrum that ranges from isolated steatosis to end-stage liver disease with fibrosis or cirrhosis, even ultimately leading to hepatocellular carcinoma(1-4). NAFLD is also closely associated with metabolic syndromes, including type II diabetes, obesity, dyslipidemia, and hypertension(5,6). The disease has been identified as a risk factor for liver surgery. Fat accumulation in the liver also affects liver regeneration in both the donor and recipient. Therefore, prompt estimation of the degree of hepatic steatosis is crucial.

To date, histopathologic analysis through liver biopsy remains the gold standard for determining and quantifying fat in the liver; however, this method is prone to sampling error(7). Furthermore, it is associated with morbidity and complications and is not suitable for continuous monitoring of the treatment response.

Imaging techniques such as computed tomography (CT) and magnetic resonance (MR) imagining enable non-invasive evaluation of the hepatic fat fraction, even when the distribution of liver fat is heterogeneous. Unenhanced CT used to be the best CT method for the assessment of hepatic steatosis because it is accurate for the semiquantitative diagnosis of macrovesicular steatosis of 30% or greater(8). These assessments are based on a simple measurement of liver attenuation(9).

More recently, dual-energy CT (DECT), in which changes in hepatic attenuation between two different energy levels can be determined by scanning with two different tube potentials, was proposed for evaluating fatty infiltration of the liver(10). Wang *et al*., who evaluated the attenuation changes between different energy levels, established that every 10% increase of liver fat content led to an increase of 4.1 HU in the attenuation difference between 90 and 120 kVp(11). Several studies found an attenuation change of at least 9 to 10 HU with a tube potential change between 140 and 80 kVp in patients with moderate hepatic Steatosis(11,12). However, further published evidence is necessary to confirm the utility of DECT for accurate quantitative assessment of liver fat infiltration using this method.

Another potential application of DECT is based on the material-differential method. In clinical practice, when materials such as iron or glycogen coexist with liver fat, the sensitivity of single-energy CT for detecting fat content is reduced(13,14). However, the new multidetector DECT can distinguish iodine, calcium, or uric acid crystals from soft tissues based on different K edge values(14,15). Despite involving exposure to ionizing radiation, DECT provides abundant data in one scan. The unique advantage of DECT is the possibility of obtaining information regarding hepatic steatosis while scanning for other abdominal diseases simply and rapidly.

For material differentiation, magnetic resonance spectroscopy (MRS) is considered the noninvasive reference standard in the quantification of hepatic triglyceride content. However, MRS requires extra post-processing effort and the quantification is performed only in a small volume of liver tissue(8). Chemical shift imaging is routinely used for estimating liver fat, but the quantification results vary with differences in MR imaging systems, scanning parameters, and analysis methods(14,16).

Thus, the main purpose of our study was to compare the diagnostic performance of spectral CT imaging, T1-weighted dual-echo chemical shift MR imaging, and 1H-MR spectroscopy (1H-MRS) in the assessment of hepatic steatosis in a fatty liver rat model, with the histopathologic result serving as the reference standard.

3. MATERIALS AND METHODS

3.1. Materials

The experimental protocols were approved by the Shanghai Ruijin Hospital Laboratory Animal Administration Committee. Fifty-one male Wistar rats (Shanghai Experimental Animal Center of Chinese Academy of Sciences, Shanghai, China) weighing approximately 281.4 ± 28.9 g were used in this study. All rats were maintained in a temperature-controlled environment with a 12:12-hour light-dark cycle. They were permitted ad libitum consumption of water and food. All rats were allowed to acclimatize for a week on the normal diet before grouping. Subsequently, the rats were randomly divided into a normal control group (n = 10) and a high-fat diet group (n = 41). The rats in the normal control group were fed normal rat pellet chow. The rats in the high-fat diet group were fed a high-fat diet composed of the following energy sources: 41% provided by carbohydrates, 40% by fat, and 19% by protein. The composition of the high-fat diet was 50% (w/w) normal food, 16.4% lard, 1% cholesterol, 17.2% sucrose, 10.4% casein, 2% premix feed, and 3% maltodextrin.

We selected seven to five rats from the high-fat diet group and two rats from the control group every 2 weeks starting at the fourth week of the experiment. The selected rats were sedated with an intraperitoneal injection of 7% chloral hydrate (0.5 mL/100 g). DECT examinations were performed with a DECT scanner (Discovery CT750 HD; GE Healthcare, Waukesha, WI). After the CT scan, the rats were transferred to the MRI scanner (3.0.T Signa MR, GE Healthcare, USA) to undergo MR scans. Immediately after the examination, the rats were euthanized with 15 ml/100 g of 7% chloral hydrate, the liver was quickly removed and perfused with saline, and the right lobe was harvested and frozen at -80 °C for further investigation.

3.2. Histology analysis

For every rat, two areas of tissue from different positions of the right lobe were submitted for hematoxylin and eosin (H&E) staining and Sudan black staining and analysis. Sudan black staining was used to quantify fat accumulation. Twelve 200× light microscopic fields were viewed on each part of tissue. An experienced pathologist (C.J, with 10 years of experience) who was blinded to the study results quantified fat accumulation by evaluating the percentage of the fat staining area for each sample in the microscopic fields by using Leica Qwin Plus software. Hepatic steatosis was also graded as follows: grade 0 (normal), less than 5%; grade 1 (mild), 5% to 33%; grade 2 (moderate), 33% to 66%; and grade 3 (severe), greater than 66%.

3.3. DECT imaging

The dual-energy scan was performed by using a GE Discovery CT750 HD (GE Healthcare) scanner with the fast kilovoltage peak (kVp) switching (80/140 kVp) Gemstone Spectral Imaging (GSI) technique. The parameters were as follows: 630 mA, 0.5-second gantry rotation time, small head scan field of view (FOV), 20-mm total coverage, and a volume CT dose index (CTDIvol) of 19.8.5 mGy. The reconstruction was processed by using GSI Viewer (AW4.4. Workstation, GE Healthcare, USA). Multiple indexes obtained from spectral CT imaging were measured, including the CT values on monochromatic images of 40 keV, effective atomic number (effective-Z),

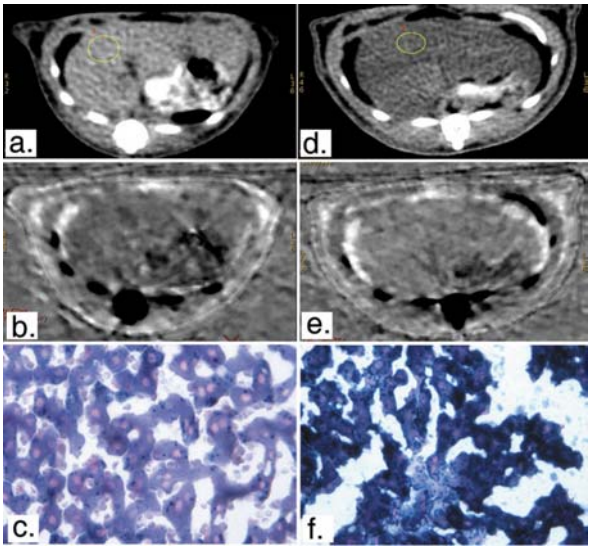

Figure 1. Figures represent coronal DECT 40keV monochromatic(a,d) and fat(water) material decomposition reformat(b,e) images with corresponding histological slides for two representative rats from normal control(a-c) and moderate fat(d-f). Circles represent the ROI Chosen.

and the fat (water) concentration (mg/ml) acquired from the fat-based material-decomposition method.

The data were processed by a resident (T.S.) under the supervision of an experienced abdominal radiologist (X.L, 13 years of experience), both of whom were blinded to the study results. We selected four CT sections of each liver for this study, while avoiding the cranial and caudal areas. A circular region of interest (ROI) of 40 mm^2 was drawn in the right lobe of the liver on each section. The distribution of four ROIs was as even as possible, while avoiding the biliary, vascular, and extrahepatic structures. Hepatic fat content was measured by using the mean index value of all ROIs in the liver.

3.4. MR imaging

T1-weighted dual-phase MR imaging and 1H-MR spectroscopy were performed by using a 3.0-T MR imager (3.0-T Signa MR, GE Healthcare, USA) with a GPFLEX coil during the same procedure (imaging time, approximately 30 minutes). MRS data were acquired using a point-resolved spectroscopy sequence with the following parameters: TR/TE, 2000/35; 64 acquisitions. Post-processing was performed using SAGE 7.0 software (GE Healthcare, USA). After identifying the water and fat resonance peaks, located at approximately 4.7 and 1.3 ppm, respectively, the area under each peak was automatically measured. The MRS hepatic fat content was calculated as follows: $[A_{1.3.\ ppm}/(A_{1.3.\ ppm} + A_{4.7.ppm})]$, with $A_{1.3.\ ppm}$ and $A_{4.7.ppm}$ representing the area under the water peak and fat peak, respectively.

A T1-weighted dual-phase sequence was acquired with the following parameters: TR/TE, 150/1.4 (out-phase) and 2.5 (in-phase); flip angle, 75°; slice thickness, 2 mm; and matrix = 256 × 128. The data were processed with AW4.4 Workstation (GE Healthcare, USA). For T1-weighted dual-echo MR imaging, four 40-mm^2 ROIs were evenly drawn in the right lobe, while avoiding other anatomic structures. The ROIs of the CT and T1-weighted dual-echo MR images were placed approximately on the same anatomical location.

The mean signal was calculated from the ROIs for each liver sample on both in-phase (SI_{IP}) and out-phase (SI_{OP}) images. The MR fat fraction (MR FF) was calculated as follows: MR FF = $(SI_{IP} - SI_{OP})/2SI_{IP}$.

All data analyses were performed by a resident (T.S.) under the supervision of an experienced MR physicist (G. N., 15 years of experience), both of whom were blinded to the study results.

3.5. Statistical analysis

All statistical analyses were performed using SPSS 13 software (SPSS version 13.0; SPSS, Chicago, IL). Spearman correlation values were used to compare the correlations between the histopathologic and imaging results. One-way analysis of variance was performed to assess the differences between groups. To select the best predictor of fatty liver grading, we also performed discriminant analysis and established a multiple regression equation of combined indexes. Receiver operating characteristic (ROC) curve analysis, including determination of cut-off values and other performance statistics, was used to determine the diagnostic performance of DECT, T1-weighted dual-echo MR imaging, and 1H-MRS in assessing hepatic steatosis. For all statistical analyses, a P value < 0.0.5 was considered to indicate a significant difference.

4. RESULTS

4.1. Correlations with histopathologic results

The DECT 40 keV monochromatic and fat (water) material-decomposition reformatted images with the corresponding histological slides are shown in Figure 1. All three DECT indexes demonstrated a strong correlation with the histopathologic examination: fat (water) concentration, r = 0.9.10 and P < 0.0.01; 40 keV monochromatic HU, r = -0.8.92 and P < 0.0.01; and effective-Z, r = -0.8.97 and P < 0.0.01. A strong correlation was also found between T1-weighted dual-echo MR imaging and histopathologic examination (r = 0.8.82 and P < 0.0.01) and between 1H-MRS and histopathologic examination (r = 0.8.94 and P < 0.0.01). The correlation coefficients with the respective P values for each modality are shown in Table 1, and the correlations are shown graphically in Figure 2.

4.2. Comparison of imaging and spectroscopic values across steatosis grades

The performances of CT, T1-weighted dual-echo MR imaging, and 1H-MRS in distinguishing different grades of steatosis are shown in Figure 3. Only 1H-MRS showed the potential to differentiate between no steatosis and mild steatosis (P = 0.0.39), mild and moderate steatosis (P < 0.0.01), and moderate and severe steatosis (P = 0.0.19).

Table 1. Pearson correlation coefficients between imaging modalities and histopathologic examination

	DECT		MR		
	40keV	Effective-Z	fat(water)	MRS HFC	MR FF
r Value	-.892	-.897	.910	.894	.882
P Value	<.001	<.001	<.001	<.001	<.001

MR FF T1-weighted dual-echo MR imaging fat fraction, MRS HFC 1H-MR spectroscopy hepatic fat content

DECT indexes and T1-weighted dual-echo MR imaging could distinguish between mild and moderate steatosis ($P < 0.0.01$) and between moderate and severe steatosis ($P < 0.0.01$), but could not differentiate between no steatosis and mild steatosis ($P = 1$).

On the basis of the histopathologic results, we evaluated the discriminant accuracy of every single index. The discriminant accuracies of the DECT indexes were 70.6% (40 keV HU), 66.7% (effective-Z), and 66.7% [fat (water)]. The MR indexes yielded discriminant accuracies of 64.7% (MR FF) and 56.9% (MRS HFC). We also established a multiple regression equation of different modalities. The combined discriminant accuracy of DECT was 78.4% [$y = -0.9.53X_1 + 5.4.93X_2 + 5.5.36X_3$, X_1 = HU (40 keV), X_2 = effective-Z, X_3 = fat (water)], while that of MR (MR FF combined with MRS HFC) was 76.5%.

4.3. Diagnostic accuracy

ROC curve fitting was performed for the indexes of DECT, T1-weighted dual-echo MR imaging, and 1H-MRS. The diagnostic performances of the three modalities are shown in Table 2, and the ROC curves of all indexes are shown in Figure 4. The cut-off value was selected to balance between sensitivity and specificity, with 5% histopathologic steatosis as the threshold value. The area under the ROC curve for the diagnosis of macrovesicular steatosis was 0.9.51 for fat (water) concentration, 0.9.68 for T1-weighted dual-echo MR imaging, and 0.9.79 for 1H-MRS, indicating that the diagnostic performances of all three modalities were acceptable. However, the performances of effective-Z and 40KeV monochromatic HU were not satisfactory.

The highest cut-off value that yielded 95.1.2% sensitivity for the diagnosis was 10.5.5% for 1H-MRS, followed by 2.7 mg/ml for fat (water) concentration with a sensitivity of 90.2.4%. The lowest sensitivity was found for T1-weighted dual-echo MR imaging (87.8.0%) with a cut-off value of 2%. The specificity was 90% for all three modalities. The positive predictive value and negative predictive value were highest for 1H-MRS (97.5% and 81.82%, respectively). These values were quite similar for T1-weighted dual-echo MR imaging and fat (water) concentration; the positive predictive value was 97.37% [fat (water) concentration] and 97.3.0% (T1-weighted dual-echo MR imaging), while the negative value was 69.2.3% [fat (water) concentration] and 64.2.9% (T1-weighted dual-echo MR imaging).

5. DISCUSSION

Our study demonstrated that DECT indexes, especially fat (water) concentration, were statistically equivalent to the findings of single-voxel MR spectroscopy and T1-weighted dual-echo MR imaging for the quantification of hepatic fat content. The fat (water) concentration, 40keV monochromatic HU, and effective-Z value showed strong statistical correlations with the histopathologic quantification results. With a threshold of 2.7 mg/ml, the sensitivity and specificity of the fat (water) concentration was 90%. The correlation also showed that the fat (water) concentration increased with an increase in fat content. The regression equation suggests that every 10% of fat content increase leads to a fat (water) increase of 71.5 mg/ml. However, this quantification result should be confirmed by further evidence in both animal models and clinical practice.

Artz *et al*., who recently published a study reporting their experience comparing DECT with chemical-shift IDEAL modality and histopathologic analysis, demonstrated excellent correlations in a phantom and *in vivo*(17). Our study, which utilized a larger number of animal models, obtained histopathologic correlation results that are similar to those reported previously, verifying the performance stability of DECT(11-14,19). Regarding the grading of hepatic steatosis, all three indexes of DECT were able to differentiate mild and moderate as well as moderate and severe hepatic steatosis, but, similar to T1-weighted dual-echo MR imaging, neither of them could differentiate normal and mild steatosis. Notably, the combined discriminant accuracy of DECT was 78.4%, indicating its potential for multiple index application. This phenomenon suggested that one or a few corrected equations would provide a higher diagnostic accuracy because a series of indexes could be obtained with DECT.

CT plays a central role in clinical practice for the screening of abdominal conditions. In recent years, the development and validation of DECT methods in abdominal diseases has been extensive(18-21). The current applications of DECT in the abdomen examinations provide an excellent opportunity to screen for hepatic steatosis in patients undergoing abdominal scans. For example, patients with endocrine system diseases, a population with a high prevalence of hepatic steatosis, may undergo scans of the pancreas. Information on the pancreas and liver steatosis can be obtained during one scan with DECT without extra scans or sequences. The strong correlation and high diagnostic performance of the material-decomposition method verified the specific ability of DECT for fat differentiation. Conditions in which materials such as iron or glycogen coexist with liver fat greatly interfere with the sensitivity of single-energy CT(22,23). Unfortunately, such conditions frequently exist in a number of diseases. DECT has been proposed for distinguishing iodine, iron, or uric acid crystals(14,21-26). Material differentiation is also important for focal fat infiltration. Intralesional fat is suggestive of hepatocellular adenoma or hepatocellular carcinoma in patients with a hepatic tumor. Despite its strong correlation in our study and in applications in previous studies(11-14,19), single keV monochromatic HU might be confounded by iron deposition, limiting its wider clinical application. Since clinical conditions may often involve circumstances that are more complicated than simple diffuse

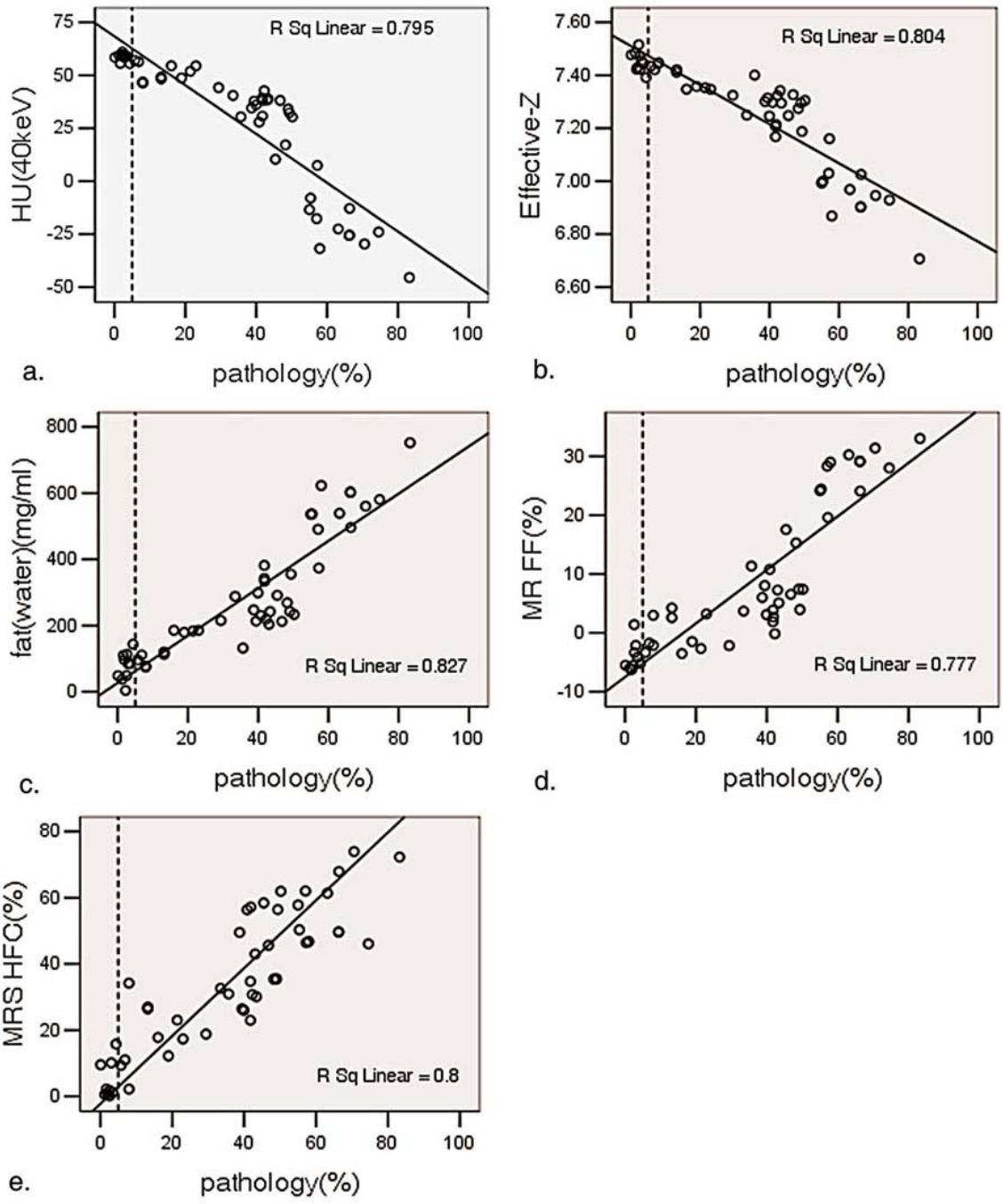

Figure 2. Scatterplot figures represent correlation between histopathologic results at (a) 40keV monochromatic HU,(b)Effective-Z value, (c) fat(water) concentration, (d) T1-weighted dual-echo MR imaging fat fraction(MR FF), and (e) 1H-MR spectroscopy hepatic fat content (MRS HFC). Dotted lines represent 5% histopathologic cut-off value.

fat infiltration in an established animal model, we believe that the material composition method is comparatively suitable for clinical use.

In this study, both T1-weighted dual-echo MR imaging and 1H-MRS showed strong correlations with the reference standard and yielded high diagnostic accuracies with good sensitivities and specificities, which is consistent with the widely held views of these techniques and with the literature(26-28). This indicates that 1H-MRS is a reproducible noninvasive technique for assessing hepatic lipid composition(29-31). Given the similar diagnostic performance of DECT and MR, we propose that DECT is a new optional quantification method. However, this

Table 2. Diagnostic accuracy of us, ct, mr imaging, and 1 h mr spectroscopy for macrovesicular hepatic fat content

	AUC	Cut-off Value	Sensitivity	Specificity	Positive Predictive Value	Negative Predictive Value	Positive Likelihood Value	Negative Likelihood Value
40keV	0.0.10							
Effective-Z	0.0.41							
fat(water)	0.9.51	2.7.049	90.2.4%	90%	97.3.7%	69.2.3%	9.0.244	0.1.084
			(37 of 41)	(9 of 10)	(37 of 38)	(9 of 13)		
MR FF	0.9.68	-0.0.214	87.8.0%	90%	97.3.0%	64.2.9%	8.7.805	0.1.355
			(36 of 41)	(9 of 10)	(36 of 37)	(9 of 14)		
MRS HFC	0.9.79	10.5.5%	95.1.2%	90%	97.5.%	81.8.2%	9.5.122	0.0.542
			(39 of 41)	(9 of 10)	(39 of 40)	(9 of 11)		

MR FF T1-weighted dual-echo MR imaging fat fraction, MRS HFC 1H-MR spectroscopy hepatic fat content

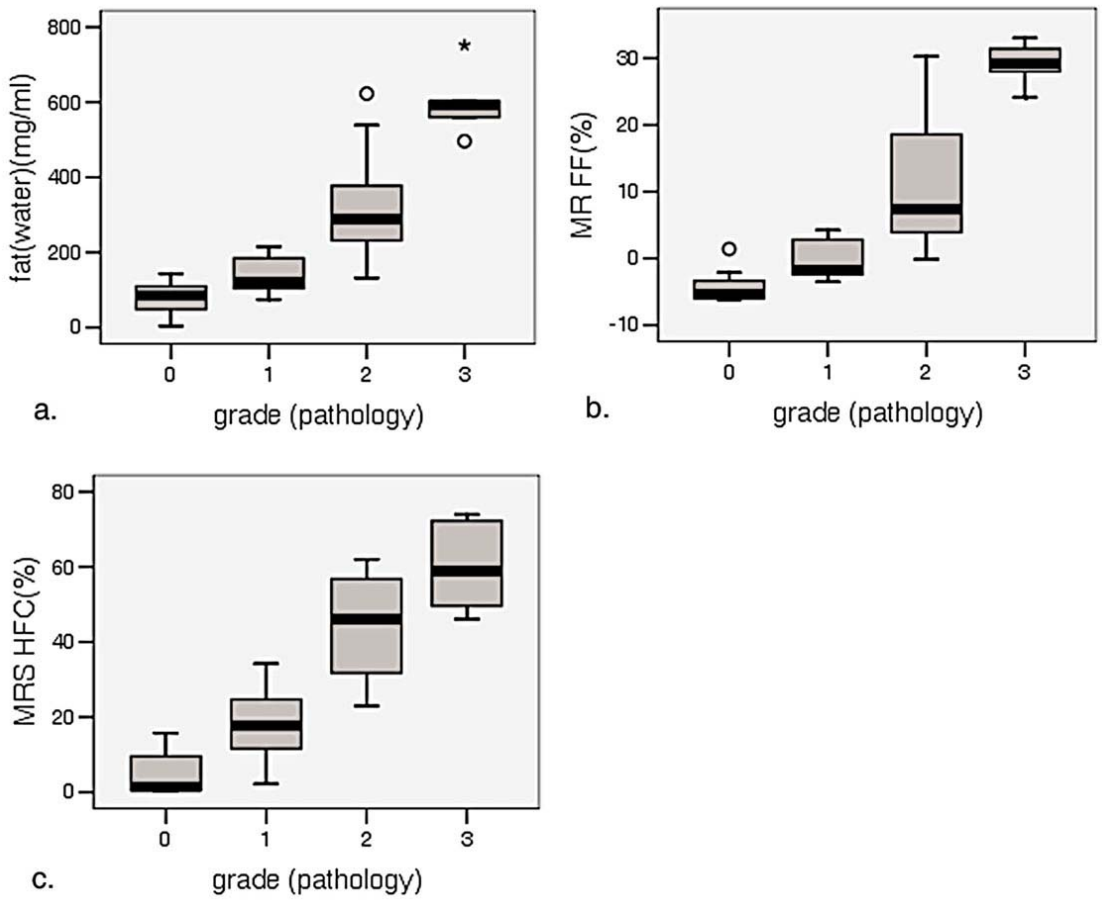

Figure 3. Boxplot figures represent performances of indexes in differentiating four stages of hepatic steatosis. (a) fat(water) concentration, (b) T1-weighted dual-echo MR imaging fat fraction(MR FF) ,(c) 1H-MR spectroscopy hepatic fat content (MRS HFC).

technique is not yet prominent enough to replace the current MR modalities fully.

This study had several limitations. First, we chose to perform 1H-MRS without breath control. The volume interrogated by 1H-MRS is blurred in the longitudinal direction by respiratory excursions of the liver, and this may lead to the relatively unstable performance of MRS compared to that observed in preliminary reports. Furthermore, the basic tissue chemical composition of the liver sample of the animal model used in this study may differ from that of human patients; thus, the cut-off value and equation obtained from the animal study should be modified in a patient study with a histopathologic correlation. Finally, a 2-point Dixon (2PD) method chemical shift sequence was utilized instead of the more advanced multi-point Dixon method or IDEAL method. However, the focus of this study was to evaluate the potential of applying DECT, and the 2PD method reportedly shows high correlations between MRS and histology, and is widely used in clinical practice(18,23,32)

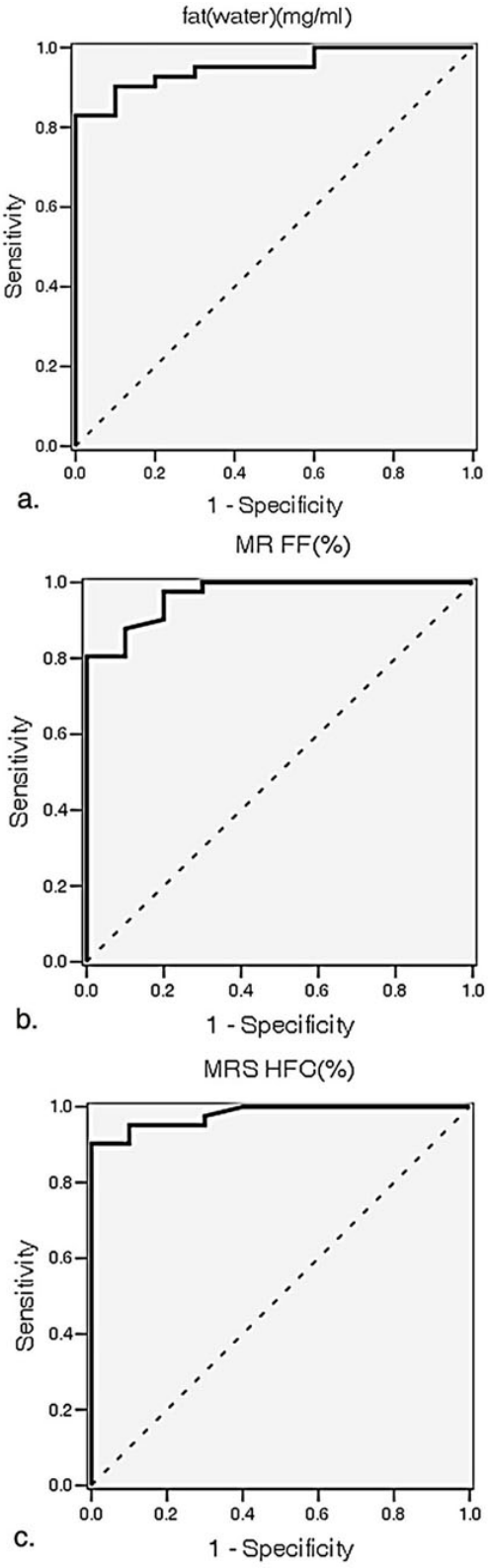

Figure 4. ROC curves represent diagnostic performance of (a) fat(water) concentration, (b) T1-weighted dual-echo MR imaging fat fraction(MR FF) and (c) 1H-MR spectroscopy hepatic fat content (MRS HFC).

6. CONCLUSION

In summary, the findings of spectral CT imaging strongly correlated with histopathologic assessments of steatosis in this study. We confirmed the ability of spectral CT imaging to provide a rapid, accurate evaluation of hepatic steatosis. The results demonstrated that the fat (water) concentration acquired from the fat-based material-decomposition method showed a stronger correlation with the reference standard and yielded a higher diagnostic accuracy than the other indexes. Further, the fat (water) concentration provided an objective assessment of steatosis, with good sensitivity and specificity. Finally, we demonstrated that the diagnostic performance of the material-decomposition method was similar to that of the T1-weighted chemical shift MR image and 1H-MRS. This encourages further exploration of the capability of DECT to quantify fat under circumstances in which the fat content coexists with iron or other compositions.

7. ACKNOWLEGMENT

The authors declared that they have no conflicts of interest to this work.

8. REFERRENCES

1. Ekstedt M, Franzén LE, Mathiesen UL, Thorelius L, Holmqvist M, Bodemar G, Kechagias S. Long-term follow-up of patients with NAFLD and elevated liver enzymes. *Hepatology*. 44 (4),865-73 (2006)

2. Starley BQ, Calcagno CJ, Harrison SA. Nonalcoholic fatty liver disease and hepatocellular carcinoma: a weighty connection. *Hepatology*. 51 (5):1820-32 (2010)

3. Guzman G, Brunt EM, Petrovic LM, Chejfec G, Layden TJ, Cotler SJ. Does nonalcoholic fatty liver disease predispose patients to hepatocellular carcinoma in the absence of cirrhosis? *Arch Pathol Lab Med*. 132 (11):1761-6 (2008)

4. Ertle J, Dechêne A, Sowa JP, Penndorf V, Herzer K, Kaiser G, Schlaak JF, Gerken G, Syn WK, Canbay A. Non-alcoholic fatty liver disease progresses to hepatocellular carcinoma in the absence of apparent cirrhosis. *Int J Cancer.* 128 (10):2436-43 (2011)

5. Adams LA, Waters OR, Knuiman MW, Elliott RR, Olynyk JK. NAFLD as a risk factor for the development of diabetes and the metabolic syndrome: an eleven-year follow-up study. *Am J Gastroenterol.* 104 (4):861-7 (2009)

6. Dunn W, Xu R, Wingard DL, Rogers C, Angulo P, Younossi ZM, Schwimmer JB. Suspected nonalcoholic fatty liver disease and mortality risk in a population-based cohort study. *Am J Gastroenterol.* 103 (9):2263-71 (2008)

7. Ratziu V, Charlotte F, Heurtier A, Gombert S, Giral P, Bruckert E, Grimaldi A, Capron F, Poynard T; LIDO Study Group. Sampling variability of liver biopsy in nonalcoholic fatty liver disease. *Gastroenterology.* 128 (7):1898-906 (2005)

8. Ma X, Holalkere NS, Kambadakone R A, Mino-Kenudson M, Hahn PF, Sahani DV. Imaging-based quantification of hepatic fat: methods and clinical applications. *Radiographics.* 29 (5):1253-77 (2009)

9. Yajima Y, Narui T, Ishii M, Abe R, Ohtsuki M, Goto Y, Endo S, Yamada K, Ito M. Computed tomography in the diagnosis of fatty liver: total lipid content and computed tomography number. *Tohoku J Exp Med.*136:337-342 (1982)

10. Raptopoulos V, Karellas A, Bernstein J, Reale FR, Constantinou C, Zawacki JK. Value of dual-energy CT in differentiating focal fatty infiltration of the liver from low-density masses. *AJR Am J Roentgenol.*157 (4):721-5 (1991)

11. Wang B, Gao Z, Zou Q, Li L. Quantitative diagnosis of fatty liver with dual-energy CT. An experimental study in rabbits. *Acta Radiol.*44 (1):92-7 (2003)

12. Mendler MH, Bouillet P, Le Sidaner A, Lavoine E, Labrousse F, Sautereau D, Pillegand B. Dual-energy CT in the diagnosis and quantification of fatty liver: limited clinical value in comparison to ultrasound scan and single-energy CT, with special reference to iron overload. *J Hepatol.* 28: 785–794 (1998)

13. Raptopoulos V, Karellas A, Bernstein J, Reale FR, Constantinou C, Zawacki JK.Value of dual-energy CT in differentiating focal fatty infiltration of the liver from low-density masses. *AJR Am J Roentgenol.* 157 (4):721-725 (1991)

14. Fischer MA, Gnannt R, Raptis D, Reiner CS, Clavien PA, Schmidt B, Leschka S, Alkadhi H, Goetti R. Quantification of liver fat in the presence of iron and iodine: an ex-vivo dual-energy CT study . *Invest Radiol.* 46 (6):351-8 (2011)

15. Graser A, Johnson TR, Bader M, Staehler M, Haseke N, Nikolaou K, Reiser MF, Stief CG, Becker CR.Dual energy CT characterization of urinary calculi: initial *in vitro* and clinical experience. *Invest Radiol.*43 (2):112-9 (2008)

16. Kim H, Taksali SE, Dufour S, Befroy D, Goodman TR, Petersen KF, Shulman GI, Caprio S, Constable RT. Comparative MR study of hepatic fat quantification using single-voxel proton spectroscopy, two-point dixon and three-point IDEAL. *Magn Reson Med.* 59 (3):521-7 (2008)

17. Artz NS, Hines CD, Brunner ST, Agni RM, Kühn JP, Roldan-Alzate A, Chen GH, Reeder SB. Quantification of Hepatic Steatosis With Dual-Energy Computed Tomography: Comparison With Tissue Reference Standards and Quantitative Magnetic Resonance Imaging in the ob/ob Mouse. *Invest Radiol.*47 (10):603-10 (2012)

18. Coursey CA, Nelson RC, Boll DT, Paulson EK, Ho LM, Neville AM, Marin D, Gupta RT, Schindera ST. Dual-energy multidetector CT: how does it work, what can it tell us, and when can we use it in abdominopelvic imaging. *Radiographics.* 30 (4):1037-55 (2010)

19. Lv P, Lin XZ, Li J, Li W, Chen K. Differentiation of small hepatichemangioma from small hepatocellular carcinoma: recently introduced spectral CT method. *Radiology.* 259 (3):720-9 (2011)

20. Zhao LQ, He W, Li JY, Chen JH, Wang KY, Tan L. Improving image quality in portal venography with spectral CT imaging. *Eur J Radiol.*81 (8):1677-81 (2012)

21. Anderson NG, Butler AP, Scott NJ, Cook NJ, Butzer JS, Schleich N, Firsching M, Grasset R, de Ruiter N, Campbell M, Butler PH. Spectroscopic (multi-energy) CT distinguishes iodine and barium contrast material in MICE. *Eur Radiol.* 20 (9):2126-34 (2010)

22. Mendler MH, Bouillet P, Le Sidaner A, Lavoine E, Labrousse F, Sautereau D, Pillegand B. Dual-energy CT in the diagnosis and quantification of fatty liver: limited clinical value in comparison to ultrasound scan and single-energy CT, with special reference to iron overload. *J Hepatol*. 28:785-794 (1998)

23. Raptopoulos V, Karellas A, Bernstein J, Reale FR, Constantinou C, Zawacki JK. Value of dual-energy CT in differentiating focal fatty infiltration of the liver from low-density masses. *Am J Roentgenol.* 157:721-725 (1991)

24. Johnson TR, Weckbach S, Kellner H, Reiser MF, Becker CR. Clinical image: dual-energy computed tomographic molecular imaging of gout. *Arthritis Rheum.* 56 (8):2809 (2007)

25. Goldberg HI, Cann CE, Moss AA, Ohto M, Brito A, Federle M. Noninvasive quantitation of liver iron in dogs with hemochromatosis using dual-energy CT scanning. *Invest Radiol.* 17 (4):375-380 (1982)

26. Primak AN, Fletcher JG, Vrtiska TJ, Dzyubak OP, Lieske JC, Jackson ME, Williams JC Jr, McCollough CH. Noninva¬sive differentiation of uric acid versus non-uric acid kidney stones using dual-energy CT. *Acad Radiol.* 14 (12):1441-1447 (2007)

27. van Werven JR, Marsman HA, Nederveen AJ, Smits NJ, ten Kate FJ, van Gulik TM, Stoker J. Assessment of hepatic steatosis in patients undergoing liver resection: comparison of US, CT, T1-weighted dual-echo MR imaging, and point-resolved 1H MR spectroscopy. *Radiology.* 256 (1):159-68 (2010)

28. Kang BK, Yu ES, Lee SS, Lee Y, Kim N, Sirlin CB, Cho EY, Yeom SK, Byun JH, Park SH, Lee MG. Hepatic fat quantification: a prospective comparison of magnetic resonance spectroscopy and analysis methods for chemical-shift gradient echo magnetic resonance imaging with histologic assessment as the reference standard. *Invest*

Radiol. 47 (6):368-75 (2012)

29. van Werven JR, Marsman HA, Nederveen AJ, ten Kate FJ, van Gulik TM, Stoker J. Hepatic lipid composition analysis using 3.0.-T MR spectroscopy in a steatotic rat model. *Magn Reson Imaging*. 30 (1):112-21 (2012)

30. Bohte AE, van Werven JR, Bipat S, Stoker J. The diagnostic accuracy of US, CT, MRI and 1H-MRS for the evaluation of hepatic steatosis compared with liver biopsy: a meta-analysis. *Eur Radiol*. 21:87-97 (2011)

31. Lee SS, Park SH, Kim HJ, Kim SY, Kim MY, Kim DY, Suh DJ, Kim KM, Bae MH, Lee JY, Lee SG, Yu ES. Non-invasive assessment of hepatic steatosis: Prospective comparison of the accuracy of imaging examinations. *J Hepatol.* 52: 579–85 (2010)

32. Westphalen AC, Qayyum A, Yeh BM, Merriman RB, Lee JA, Lamba A, Lu Y, Coakley FV. Liver fat: effect of hepatic iron deposition on evaluation with opposed-phase MR imaging. *Radiology*. 242:450-455 (2007)

Key Words: Steatosis, Dual-Energy Ct, Mrs,Chemical-Shift Mr, Quantification

Send correspondence to: Ke-min Chen, No, 197 Ruijin Er Rd, Shanghai, 200011, China, Tel: 86-21-13917117665, Fax: 86-21-64370045, E-mail: graciass@gmail.com